A Multi-focus Image Fusion Method Based on Linear Canonical Transform

Yan-An Xie
School of Information and Electronics
Beijing Institute of Technology
Beijing, China 100081
Email: shy1976@bit.edu.cn

Yong Guo
School of Mathematics and Statistics
Beijing Institute of Technology
Beijing, China 100081
Email: nmbtgygy@126.com

Bing-Zhao Li
School of Mathematics and Statistics
Beijing Institute of Technology
Beijing, China 100081
Email: li_bingzhao@bit.edu.cn

***Abstract*—In this paper, the self-linear canonical functions (SLCFs) based on linear canonical transform (LCT) are discussed and proposed. We found that the SLCFs can be used to decompose an image into M complex images. Based on this property, a novel multi-focus image fusion method is proposed in this paper. The simulations are carried out to show the importance of parameters in application of the SLCFs decomposition. According to the simulation results, the proposed fusion method with appropriate parameters can improve the quality of fused images.**

***Index Terms*—Image fusion, self-linear canonical functions, multi-focus image, discrete cosine transform, discrete sine transform**

I. Introduction

Image fusion can be defined as a process in which a new image is produced by integrating complementary, multi-focus or multi-view information from a set of source images. Nowadays, the image fusion has been widely used in machine vision, object recognition, medical imaging and military affairs. The image fusion process can be performed at different level of information representation, namely pixel level, feature level and decision level [1]. Pixel level image fusion is the lowest level fusion, but it has higher accuracy and more detail information than other fusion levels.

Basically, the pixel level fusion methods can be divided into two categories. The first category is the spatial domain-based methods which directly select pixels or regions from clear parts in the spatial domain to compose fused images [2]–[8], such as nonlinear weighed multi-band fusion image algorithm [2], region segmentation and spatial frequency fusion method [3]. The second category is the transform domain based methods which fuse images using time-frequency transform [9]–[16], such as the image fusion algorithms based on discrete wavelet transform (DWT) [9]–[12], discrete cosine transform (DCT) [13]–[15] and fractional Fourier transform (FRFT) [16].

Multi-focus image fusion is a typical application for pixel level image fusion. Due to the limited depth of focus of optical lenses, it is impossible to get an image which contains all relevant objects in focus. One possibility to overcome this problem is to take several pictures with different focus points and combine them together into a single frame which finally contains the focused regions of all input images. The transform domain methods are mainly used in the multi-focus image fusion.

As a new kind of time-frequency transform, the linear canoncial transform (LCT) is actively used in optics, quantum theory, signal and image processing [17], [18]. The self-linear canonical functions (SLCFs) based on LCT is proposed by T. Alieva in [19] to investigate the self-imaging phenomenon in first-order optical systems. Until recently, to the best of our knowledge, there is no research paper has been published about image fusion based on the SLCFs decomposition. Therefore, it is interesting and worthwhile to explore the image fusion methods associated with the theory of SLCFs.

II. Self-linear canonical functions

A. Linear Canonical Transform

The continuous LCT with real parameter matrix A of a signal $f(x,y)$ is defined as

$$F_A(u,v) = R^A[f(x,y)](u,v) = \int_{R^2} f(x,y)K_A(x,u)K_A(y,v)dxdy \tag{1}$$

with the kernel

$$K_A(x,u) = \begin{cases} \dfrac{1}{\sqrt{ib}}\exp(i\pi\dfrac{ax^2+du^2-2xu}{b}), b\neq 0, \\ \dfrac{1}{\sqrt{a}}\exp(i\pi\dfrac{cu^2}{a})\delta(u-x/a),\ b=0, \end{cases} \tag{2}$$

where $A=\begin{pmatrix} a & b \\ c & d \end{pmatrix}$ satisfying $ad-bc=1$, R^A is the LCT operator and F_A is the LCT of $f(x,y)$.

When $b\neq 0$, let $a=\gamma/\beta, b=1/\beta, c=-\beta+\alpha\gamma/\beta, d=\alpha/\beta$. The kernel of LCT with three parameters α,β,γ can be written as

$$K_A(x,u) = \sqrt{\beta}\exp(-\frac{i\pi}{4})\exp[i\pi(\alpha u^2-2\beta xu+\gamma x^2)]. \tag{3}$$

There several kinds of discrete LCT algorithms proposed in [22]–[24]. The discrete LCT of a size $P\times Q$ image $I(p,q)$ is defined as [23]

$$F_A(u,v) = \sum_{q=1}^{Q} C_A^Q(v-1,q-1)\sum_{p=1}^{P} C_A^P(u-1,p-1)I(p,q), \tag{4}$$

978-1-5090-2708-8/16/$31.00 ©2016 IEEE

where $C_A^Q(v-1,q-1)$ and $C_A^P(u-1,p-1)$ have the same form as follows

$$C_A^N(x,y) = \frac{\sqrt{\beta}\exp(-i\pi/4)}{\sqrt{N|\beta|}}\exp[\frac{i\pi}{N|\beta|}(\alpha x^2 - 2\beta xy + \gamma y^2)] \quad (5)$$

B. Self-linear Canonical Functions

The self-linear canonical function (SLCF) $f(x,y)$ is a function such that $R^A f(x,y) = c_0 f(x,y)$, where $c_0 = \exp(-i2\pi\varphi)$ is a complex constant and R^A is the LCT operator.

As it follows from Parserval's relation for the LCT of a signal with finite energy $\int |f(x,y)|^2 dxdy < \infty$, we can get $|c_0| = 1$ and φ is real. It has been shown that the functions

$$\psi_n(x) = (\sqrt{\pi}2^n n!)^{-1/2}\exp(-\frac{1+i\xi}{2\lambda^2}x^2)H_n(x/\lambda) \quad (n \in N)$$

are eigenfunctions for the one-dimensional LCT with eigenvalue $c_1 = \exp(-i(n+1/2)\theta)$, where $H_n(u)$ are the Hermite polynomials, θ, λ and β are respectively defined as following

$$\begin{gathered}\theta = \arccos(\frac{a+d}{2}), \lambda^2 = 2b(4-(a+d)^2)^{-1/2} \\ \xi = (a-d)(4-(a+d)^2)^{-1/2}\end{gathered} \quad (6)$$

In this paper, it is worthy to point out that the condition $|a+d| < 2$ is supposed and thus these parameters θ, λ and ξ are real under this condition. In this case, the following two theorems of the SLCF are interesting.

Theorem 1. *Any function $f(x,y)$ from $L^2(R^2)$ can be decomposed into M SLCFs $g(x,y)_{M,L}(L = 0,1,\cdots,M-1)$ as follows*

$$f(x,y) = \sum_{L=0}^{M-1} g(x,y)_{M,L}, \quad (7)$$

where M is positive integer and $g(x,y)_{M,L}$ is SLCFs.

Proof: Due to the fact that the functions $\psi_n(n \in N)$ form a complete orthogonal set, any function from $L^2(R)$ can be represented as a linear combination of $\psi_n(n \in N)$. Let $f(x,y)$ be any function from $L^2(R^2)$, then we can represent $f(x,y)$ as the following form

$$f(x,y) = \sum_{m=0}^{\infty}\sum_{n=0}^{\infty} f_{m,n}\psi_m(x)\psi_n(y), \quad (8)$$

Let $m = j_x M + m_0$, $n = j_y M + n_0$, $m_0 + n_0 = L$, where j_x and j_y are non-negative integers, $m_0 \in D_M = \{z \mid z \text{ is a integer from the interval } [0,M] \text{ such that } L - m_0 \geq 0\}$. Thus, the final result can be obtained as formula shown in Eq. (9). ∎

Theorem 2. *Suppose* $A = \begin{pmatrix} \cos\theta + \xi\sin\theta & \lambda^2\sin\theta \\ -(\xi^2+1)\lambda^{-2}\sin\theta & \cos\theta - \xi\sin\theta \end{pmatrix}$ *satisfying $\theta = \arccos(\frac{a+d}{2}) = 2\pi/M$, then a self linear canonical function with parameter matrix A can be constructed from any generator function $f(x,y)$ as the following form*

$$g(x,y)_{M,L} = \frac{1}{M}\sum_{k=1}^{M}\exp(\frac{i2\pi(L+1)(k-1)}{M})[R^{A^{k-1}}f(u,v)]. \quad (11)$$

Proof: Let $\theta = 2\pi/M, m = j_x M + m_0$, $n = j_y M + L - m_0$, $j = j_x + j_y$, then the result can be given by Eq. (10) ∎

III. Fusion method

In this section, we present a novel image fusion method based on LCT. Firstly, the source image $f_i(x,y)$ can be decomposed into M complex images $g_i(x,y)_{M,L}(L = 0,1,\cdots,M-1)$ with parameters λ, ξ and θ, which can be expressed as

$$f_i(x,y) = \sum_{L=0}^{M-1} g_i(x,y)_{M,L} \quad (12)$$

where

$$g_i(x,y)_{M,L} = \frac{1}{M}\sum_{k=1}^{M}\exp(\frac{i2\pi(L+1)(k-1)}{M})[R^{A^{k-1}}f_i(u,v)] \quad (13)$$

are SLCFs and $i = 1,2$. Secondly, each $g_i(x,y)_{M,L}$ can be acted by a transform, such as DCT and discrete sine transform (DST), where the transform is denoted as $T[\cdot]$. Thirdly, maximum absolute value fusion rule applied for $T[g_i(x,y)_{M,L}]$ to obtain $T[g(x,y)_{M,L}]$. Finally, in order to get $g(x,y)_{M,L}$, we apply inverse transform on $T[g(x,y)_{M,L}]$ and the final fused image $f(x,y)$ is given by

$$f(x,y) = \sum_{L=0}^{M-1} g(x,y)_{M,L}. \quad (14)$$

The above procedure can be summarized in following steps:

Step 1: The source images $f_i(x,y)$ are decomposed into M complex images $g_i(x,y)_{M,L}(i = 1,2$ and $L = 0,1,\cdots,M-1)$.

Step 2: Each image $g_i(x,y)_{M,L}$ is then transformed by $T[\cdot]$ to obtain transform coefficient $T[g_i(x,y)_{M,L}]$.

Step 3: Apply the maximum absolute value fusion rule on the each $T[g_i(x,y)_{M,L}]$ $(i = 1,2)$ to obtain $T[g(x,y)_{M,L}]$.

Step 4: Apply $T^{-1}[\cdot]$ on the $T[g(x,y)_{M,L}]$, then the final fused image can be obtained by Eq. (14).

IV. Results and analysis

All experiments are conducted on a personal computer having Intel dual core 3.2 GHz CPU with 4.0 GB RAM, and using MATLAB version R2014a under the Windows 7 environment. In this section, two 512 × 512 multi-focus images are used as the source images, which are shown in Fig. 1 (a) and (b) respectively. Reference images are shown in Fig. 1 (c), where all objects are focus.

(a) Focus on the right (b) Focus on the left (c) Reference image

Fig. 1. The 'clock' source images

SLCFs decomposition combined with DCT (abbreviated as SLCFs+DCT) and SLCFs decomposition combined with DST (abbreviated as SLCFs+DST) are used to display the

$$f(x,y)=\sum_{m_0=0}^{M-1}\sum_{n_0=0}^{M-1}(\sum_{m_0\in D_M}\sum_{j_x=0}^{\infty}\sum_{j_y=0}^{\infty}f_{m_0+j_xM,L-m_0+j_yM}\psi_{m_0+j_xM}(x)\psi_{L-m_0+j_yM}(y)=\sum_{m_0=0}^{M-1}\sum_{n_0=0}^{M-1}g(x,y)_{M,L}=\sum_{L=0}^{M-1}g(x,y)_{M,L} \tag{9}$$

where $g(x,y)_{M,L}=\sum_{m_0\in D_M}\sum_{j_x=0}^{\infty}\sum_{j_y=0}^{\infty}f_{m_0+j_xM,L-m_0+j_yM}\psi_{m_0+j_xM}(x)\psi_{L-m_0+j_yM}(y)$.

$$\begin{aligned}
g(x,y)_{M,L}&=\sum_{m_0\in D_M}\sum_{j_x=0}^{\infty}\sum_{j_y=0}^{\infty}f_{m_0+j_xM,L-m_0+j_yM}\psi_{m_0+j_xM}(x)\psi_{L-m_0+j_yM}(y)\\
&=\frac{1}{M}\sum_{m=0}^{\infty}\sum_{n=0}^{\infty}f_{m,n}\psi_m(x)\psi_n(y))\sum_{k=1}^{M}\exp(\frac{i2\pi[L-(n+m)](k-1)}{M})\\
&=\frac{1}{M}\sum_{k=1}^{M}\exp(\frac{i2\pi(L+1)(k-1)}{M})\sum_{m=0}^{\infty}\sum_{n=0}^{\infty}\exp(\frac{-i2\pi(n+m+1)(k-1)}{M})f_{m,n}\psi_m(x)\psi_n(y))\\
&=\frac{1}{M}\sum_{k=1}^{M}\exp(\frac{i2\pi(L+1)(k-1)}{M})[R^{A^{k-1}}(\sum_{m=0}^{\infty}\sum_{n=0}^{\infty}f_{m,n}\psi_m(x)\psi_n(y))]\\
&=\frac{1}{M}\sum_{k=1}^{M}\exp(\frac{i2\pi(L+1)(k-1)}{M})[R^{A^{k-1}}f(u,v)](x,y).
\end{aligned} \tag{10}$$

simulation experiment. Since the SLCFs decomposition has the parameters M, λ and ξ, so it is necessary to consider the effectiveness of those parameters on the quality of fused images. In simulation experiment, we first consider parameter M as variation when λ and ξ are fixed. Similarly, we perform experiments for the parameter λ and ξ as variations. In addition, it is worthy to note that we apply the maximum absolute value fusion rule to obtain the better quality of fused images and the fusion method based on DWT is used as a comparison to show the advantages of the proposed method.

A. The Sensitivity Analysis of Parameters

Firstly, taking Fig. 1 as an example and letting $\lambda = 1$, $\xi = 2$, fuse methods are SLCFs+DCT and SLCFs+DST.

Because human subjective visual perception is easily influenced by psychological factors, objective evaluation criteria are commonly used to evaluate the quality of the fused images, such as standard deviation (STD), information entropy (IE), mutual information (MI), edge retention $Q^{AB/F}$ and root mean square error (RMSE) [25], where STD and IE do not require the reference image. RMSE reflects the difference degree between the fused image and reference image. STD reflects the gray value of the image deviation degree to mean gray. IE describes the amount of information contained in an image. MI is defined as the sum of mutual information between each reference image and the fused image, which is used for describe the average information of fused image. The index $Q^{AB/F}$ measures the amount of edge information transferred from the source images to the final fused image using a sobel edge detector, which reflects the structural similarity degree between the fused image and reference images. The MI, IE, STD, RMSE and $Q^{AB/F}$ values are listed in Table I and Table II.

TABLE I
THE OBJECTIVE EVALUATION OF SLCFS+DCT WITH VARIOUS M FOR CLOCK

Parameters	STD	RMSE	IE	MI	$Q^{AB/F}$
M=3	40.8566	21.6668	0.0589	3.6413	0.4379
M=4	41.2031	21.3853	0.1235	3.7565	0.4941
M=5	40.7502	21.7265	0.0458	3.6101	0.4315
M=6	40.9368	21.5797	0.0570	3.6247	0.4502
M=7	40.6674	21.8016	0.0454	3.6307	0.4251
M=8	40.7925	21.6788	0.0473	3.6547	0.4446
M=9	40.6079	21.8652	0.0439	3.6259	0.4157

TABLE II
THE OBJECTIVE EVALUATION OF SLCFS+DST WITH VARIOUS M FOR 'CLOCK' IMAGE

Parameters	STD	RMSE	IE	MI	$Q^{AB/F}$
M=3	40.0026	22.4847	0.0672	3.7147	0.3980
M=4	40.3328	22.2891	0.1227	3.7721	0.4553
M=5	39.9396	22.4841	0.0543	3.6766	0.4016
M=6	39.9815	22.5639	0.0576	3.6584	0.4040
M=7	39.8942	22.4837	0.0526	3.6752	0.4009
M=8	39.9751	22.0134	0.0546	3.6555	0.4175
M=9	39.8497	22.5284	0.0496	3.6764	0.3964

Obviously, four level of decomposition provide the lower values of RMSE. The lower values of RMSE are, the better quality of fused image is. Thus, it means that the fused image using the parameter $M = 4$ has lower difference compared with reference image. Meanwhile four levels of decomposition provide the higher values of MI, IE, STD and $Q^{AB/F}$. For MI, IE, STD and $Q^{AB/F}$, larger values indicate the better quality of fused image. Thus, these values reflect that the fused image using the parameter $M = 4$ have higher performance than those images using other M listed in Table I. Based on the above analysis, the fused images using $M = 4$ are better than those images using other M, they are shown in Fig. 2 (a) and (b). Compared with the source image Fig. 1 (a) and (b), the quality

of fused images based on both SLCFs+DCT and SLCFs+DST are greatly improved, especially the fusion method based on SLCFs+DCT is encouragement.

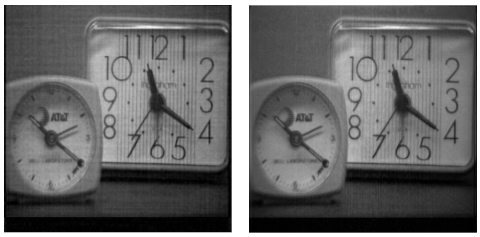

(a) SLCFs+DCT (b) SLCFs+DST

Fig. 2. The 'clock' fused image using the parameter $\lambda = 1, \xi = 2, M = 4$

Secondly, fix $M = 4$, λ and ξ are selected as variation to obtain the fused images using 'clock' source images and SLCFs+DCT. Taking $\lambda = -10, -5, -1, 1, 5, 10$ as six examples, the values of MI, IE, STD, RMSE and $Q^{AB/F}$ are listed in Table III. It can be seen from the Table III that the quality of fused images are not influenced by λ. Furthermore, the five criteria of fused image using $\xi = -5, -4, -3, -2, -1, 1, 2, 3, 4, 5$ are listed in Table IV. By examining Table IV, it can be seen that the values of MI, IE, STD, RMSE and $Q^{AB/F}$ of fused image are symmetrical on ξ.

TABLE III
THE OBJECTIVE EVALUATION OF SLCFS+DCT WITH VARIOUS λ FOR CLOCK

Parameters	STD	RMSE	IE	MI	$Q^{AB/F}$
λ=-10	41.2031	21.3853	0.1235	3.7565	0.4941
λ=-5	41.2031	21.3853	0.1235	3.7565	0.4941
λ=-1	41.2031	21.3853	0.1235	3.7565	0.4941
λ=1	41.2031	21.3853	0.1235	3.7565	0.4941
λ=5	41.2031	21.3853	0.1235	3.7565	0.4941
λ=10	41.2031	21.3853	0.1235	3.7565	0.4941

TABLE IV
THE OBJECTIVE EVALUATION OF SLCFS+DCT WITH VARIOUS ξ FOR CLOCK

Parameters	STD	RMSE	IE	MI	$Q^{AB/F}$
ξ=-5	41.2603	21.3390	0.1244	3.7529	0.4922
ξ=-4	41.1802	21.3801	0.1251	3.7650	0.4940
ξ=-3	41.2405	21.3569	0.1188	3.7399	0.4891
ξ=-2	41.2031	21.3853	0.1235	3.7565	0.4941
ξ=-1	41.1399	21.3562	0.0756	3.7458	0.4900
ξ=1	41.1399	21.3562	0.0756	3.7458	0.4900
ξ=2	41.2031	21.3853	0.1235	3.7565	0.4941
ξ=3	41.2405	21.3569	0.1188	3.7399	0.4891
ξ=4	41.1802	21.3801	0.1251	3.7650	0.4940
ξ=5	41.2603	21.3390	0.1244	3.7529	0.4922

B. Cross Comparison

The fusion method based on discrete wavelet transform (DWT) is classical fusion method. In order to show advantages of the proposed method, the method is compared with the fusion method using DWT. The 'rbio 2.2' wavelet and 'bior 1.5' wavelet, together with decomposition level of 2, are used in the DWT-based method. The fused images based on different methods are shown in Figure 3. The five criteria of fused image using different methods are listed in Table V. Through the comparison of data, we can find that the fusion method using SLCFs+DCT are better than fusion method using DWT on STD, RMSE, IE and $Q^{AB/F}$.

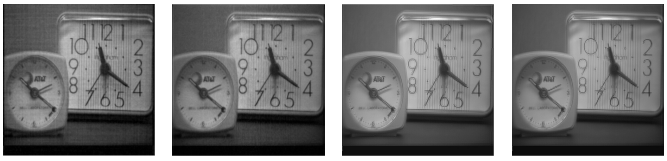

(a) SLCFs+DCT (b) SLCFs+DST (c) DWT rbio2.2 (d) DWT bior1.5

Fig. 3. The 'clock' fused images using different methods

TABLE V
THE OBJECTIVE EVALUATION OF FUSED IMAGES WITH VARIOUS METHODS

Methods	STD	RMSE	IE	MI	$Q^{AB/F}$
SLCFs+DCT	41.2031	21.3853	0.1235	3.7565	0.4941
SLCFs+DST	40.3328	22.2891	0.1227	3.7721	0.4553
DWT rbio2.2	40.3640	22.0932	0.0434	4.3726	0.4719
DWT bior1.5	40.6800	21.6440	0.1351	4.5633	0.4832

V. CONCLUSION

In this paper, the SLCFs based on the LCT are proposed and they can be used to decompose an image into M complex images. Therefore, we apply the SLCFs decomposition into image fusion. According to the simulation results, the fusion method using parameter $M = 4$ can obtain better quality of fused image. The parameter λ do not affect the performance of fused images, while the proposed method using some ξ can improve the values of MI, IE, STD, RMSE and $Q^{AB/F}$. It means that M and ξ are the key factors for the quality of fused images. Finally, the proposed methods are compared with the fusion method using DWT, the fusion method using SLCFs+DCT are better than fusion method using DWT on STD, RMSE, IE and $Q^{AB/F}$.

REFERENCES

[1] Z. Zhang and R. S. Blum, " A categorization of multiscale decomposition based image fusion schemes with a performance study for a digital camera application," Proceeding of IEEE, vol. 87, no. 8, pp. 1315-1326, 1999.

[2] R. Fan, Q. Yang and G. Liu, "Nonlinear weighted multiband fusion image algorithm," Electronics, Computer and Applications, 2014 IEEE Workshop on. IEEE, pp. 449-452, 2014.

[3] S. Li and B. Yang, "Multifocus image fusion using region segmentation and spatial frequency," Image and Vision Computing, vol. 26, no. 7, pp. 971-979, 2008.

[4] G. Piella, "A general framework for multiresolution image fusion: from pixels to regions," Information fusion, vol. 4, no. 4, pp. 259-280, 2003.

[5] Y. Zhang and L. Ge, "Efficient fusion scheme for multi-focus images by using blurring measure," Digital Signal Processing, vol. 19, no. 2, pp. 186-193, 2009.

[6] G. Salvador and C. Gabriel, " On the use of a joint spatial-frequency representation for the fusion of multi-focus images," Pattern Recognition Letters, vol. 26, no. 16, pp. 2572-2578, 2005.

[7] S. T. Li, J. T. Kwok and Y. N. Wang, "Combination of images with diverse focuses using the spatial frequency," Information Fusion, vol. 2, no. 3, pp. 169-170, 2001.

[8] N. Cvejic, D. Bull and N. Canagarajah, "Region-based multimodal image fusion using ICA bases," IEEE Sensors Journal, vol. 7, no. 5, pp. 743-751, 2007.
[9] T. Ranchin and L. Wald, "The wavelet transform for the analysis of remotely sensed images," International Journal of Remote Sensing, vol. 14, no. 3, pp. 615-619, 1993.
[10] I. Mehra and N. K. Nishchal, "Image fusion using wavelet transform and its application to asymmetric cryptosystem and hiding," Optics express, vol. 22, no. 5, pp. 5474-5482, 2014.
[11] R. Singh and A. Khare, "Fusion of multimodal medical images using Daubechies complex wavelet transformCA multiresolution approach," Information Fusion, vol. 19, pp. 49-60, 2014.
[12] R. R. Singh and R. MISHRA, "Benefits of Dual Tree Complex Wavelet Transform over Discrete Wavelet Transform for Image Fusion," International Journal for Innovative Research in Science and Technology, vol. 1, no. 11, pp. 259-263, 2015.
[13] Y. A. V. Phamila and R. Amutha, "Discrete Cosine Transform based fusion of multi-focus images for visual sensor networks," Signal Processing, vol. 95, pp. 161-170, 2014.
[14] L. Cao, L. Jin and H. Tao, et al., "Multi-focus image fusion based on spatial frequency in discrete cosine transform domain," Signal Processing Letters, IEEE, vol. 22, no. 2, pp. 220-224, 2015.
[15] V. P. S. Naidu, "Discrete cosine transform-based image fusion," Defence Science Journal, vol. 60, no. 1, pp. 48-54, 2010.
[16] K. K. Sharma and M. Sharma, "Image fusion based on image decomposition using self-fractional Fourier functions," Signal, image and video processing, vol. 8, no. 7, pp. 1335-1344, 2014.
[17] T. Z. Xu and B. Z. Li, *Linear Canonical Transformations and Its Applications*, Beijing, Science Press, 2013.
[18] W. Qiu, B. Z. Li and X. W. Li, "Speech recovery based on the linear canonical transform," Speech Communication, vol. 55, no. 1, pp. 40-50, 2013.
[19] M. J. Bastiaans, "Properties of eigenfunctions of canonical integral transform," NSIP, pp. 585-587, 1999.
[20] D. Mendlovic, H. M. Ozaktas and A. W. Lohmann, "Self Fourier functions and fractional Fourier transforms," Optics communications, vol. 105, no. 1, pp. 36-38, 1994.
[21] T. Alieva and A. M. Barb, "Self-fractional Fourier functions and selection of modes," Journal of Physics A: Mathematical, Nuclear and General, vol. 30, no. 8, pp. L211-L215, 1997.
[22] S. C. Pei and J. J. Ding, "Eigenfunctions of linear canonical transform," Signal Processing, IEEE Transactions on, vol. 50, no. 1, pp. 11-26, 2002.
[23] A. Koc, H. M. Ozaktas and C. Candan, "Digital computation of linear canonical transforms" IEEE Transactions on Signal Processing, vol. 56, no. 6, pp. 2383-2394, 2008.
[24] J. J. Healy and J. T. Sheridan, "Sampling and discretization of the linear canonical transform," Signal Processing, vol. 89, no. 4, pp. 641-648, 2009.
[25] C. S. Xydeas and V. Petrovic, "Objective image fusion performance measure," Electronics Letters, vol. 36, no. 4, pp. 308-309, 2000.